Neuron Guidance and Nano-Neurosurgery Using Optical Tools

Manoj V. Mathew

Barcelona, June, 2009

Universitat Politècnica de Catalunya

ICFO - Institut de Ciències Fotòniques

*Doctorate Program:***Photonics**

Duration: **2005-2009.**

Thesis advisor: **Dr. Pablo Loza-Alvarez**

Thesis submitted in partial fulfilment of the requirements for the degree of Doctor of Philosophy of the Technical Universtiy of Catalunya

June 2009

dedicated to my mother

I have spent my days stringing and unstringing my instrument while the song I came to sing remains unsung.

– **Ravindranath Tagore**
(Nobel Laureate)

Acknowledgment

I am grateful to ICFO-The institute of photonic sciences for giving me the opportunity to pursue my doctoral research in a very exciting field of investigation. I am also extremely grateful to Department of Innovation, Universities and Enterprises of the Catalan Government and European Social Fund for my FI pre-doctoral fellowship and the BE-AGUAR-2008 fellowship for travel abroad. Thanks also goes to Department of Cell and Molecular Biology, Gothenburg University, which hosted my 5 months research stay. There are a large number of individuals, without whom this thesis would not have been possible. I would like to sincerely thank each and every one of them, without naming anyone individually. Thank you all.

Abstract

In recent years light has emerged as a very powerful tool in the biomedical field for investigation, diagnosis as well as therapies. The field of neuroscience and medical neurology has also benefited immensely form use of these photonic tools. Axon guidance for example has been achieved by the use of CW light in contact with growth cones by exploiting light's ability to impart forces.

Following this line of research our investigation revealed the potential of a pulsed laser light placed at a distance to induce a signaling effect and hence attraction in axons of cortical neurons *in-vitro*. Laser light was focused through a microscope objective to a point placed at a distance of about 15μm from the growth cone. The experiments were performed using continuous wave (CW), chopped CW (20Hz) and modelocked fs (FS) laser beams (80MHz) with 3mW of average power at the sample plane. In addition, a sham situation (no light beam) was used as a control. We found that CW light does not produce any significant influence on the axon growth. In contrast, when using pulsed light (chopped CW light or FS pulses), the beam was able to modify the trajectory of the axons, attracting approximately 45% of the observed cases to the beam spot. These results show that pulsed NIR laser light is capable of modulating the growth of axons in living cultured neurons. In the long term, this optically-based method has the potential to open up new alternatives to guide axons and in the search for therapies for neural degenerative disorders and injuries.

In order to exploit similar optically induced effects *in-vivo* a new optical tool the multimodal optical workstation was developed. The basic motivation behind building this system was the development of a tool that could induce optical stimulation and at the same time image the results of stimulation live, using a multitude of imaging modalities. The workstation extends a commercially available confocal microscope (Nikon Confocal C1-Si) to include nonlinear/multiphoton microscopy and optical manipulation/stimulation tools such as nanosurgery. The setup allows both subsystems (confocal and nonlinear) to work independently and simultaneously. The workstation enables, for instance, confocal fluorescence microscopy, Laser Scanning Bright Field (LSBF) imaging and Second Harmonic Generation (SHG) imaging to be performed at the same time. The nonlinear microscopy capabilities are added around the commercial confocal microscope by exploiting all the flexibility offered by this microscope and without need for any mechanical or electronic modification of the confocal microscope systems.

The multimodal optical workstation was used for performing Nano-neurosurgery and observing the dynamics associated with the procedure by multimodal imaging of the procedure live, using a multitude of imaging modalities. A number of effects that happen along with the process of nanosurgery, like spilling of axoplasm, laser induced muscular contraction etc: were observed. A through assessment of collateral damage could also be performed. The ability of the multimodal system to assess collateral damage is much superior to the currently established ways of detecting collateral damage after Nano-neurosurgery. In addition SHG microscopy was introduced as a novel technique to detect collateral damage to the muscle surrounding the neurite targeted for Nano-neurosurgery.

Resumen

En los últimos años, la luz ha emergido como poderosa herramienta en la investigación biomédica tanto como para el diagnóstico de enfermedades como en terapias. Los campos de la neurociencia y la neurología también se han beneficiado enormemente del uso de las diversas herramientas fotónicas. Por ejemplo, se ha conseguido guiado axonal utilizando fuentes de luz continua cuando la luz entra en contacto con conos de crecimiento axonales, explotando así su habilidad para impartir fuerzas.

Siguiendo esta línea de trabajo, nuestra investigación ha hecho evidente el potencial que tiene la luz láser para inducir, a distancia, un efecto de señalización capaz de atraer axones de neuronas corticales cultivadas *in-vitro*. En este caso, la luz láser se fue enfocada a una distancia de aproximadamente 15μm del cono de crecimiento axonal. Los experimentos fueron llevados a cabo utilizando luz continua (CW), luz modulado con un "chopper" mecánico a 20Hz (chopped CW) y luz de un oscilador láser de pulsos ultracortos operando a 80MHz (FS). En todos los casos se utilizó una potencia promedio de 3mW medidos en el plano de la muestra. Adicionalmente, experimentos de control (sham) fueron realizados. En estos no había ningún haz de luz láser incidiendo sobre la muestra. Se encontró que la luz CW no produce ningún efecto significativo sobre los conos de crecimiento. Sin embargo, cuando se utilizó luz pulsada (chopped CW o FS), se encontró que el haz era capaz de modificar la trayectoria de los axones atrayendo aproximadamente al 45% de ellos. Estos resultados indican que la luz es capaz de modular el crecimiento de neuronas cultivadas *in-vitro*. A largo plazo, este método óptico tiene el potencial de conseguir guiado de axones y, por lo tanto, de abrir nuevas opciones en la búsqueda de terapias capaces de remediar, por ejemplo, accidentes cerebrales y enfermedades neurodegenerativas.

Para explotar los efectos inducidos ópticamente *in-vivo*, nuevas herramientas ópticas tuvieron que ser desarrolladas. Una de ellas consiste en la estación de trabajo de microscopía multimodal. Esta herramienta fue construida con el objetivo de ser capaces de poder estimular ópticamente las neuronas, al mismo tiempo que se realizaba la visualización de las neuronas bajo estos estímuls con varias modalidades de microscopa. La estacin de trabajo se construyó a partir de un microscopio confocal comercial (Nikon Confocal C1-Si) y permitió, de una manera sencilla, incluir diferentes métodos de microscopa no lineal o de multifotón, ademós de incorporar otras herramientas de manipulación/estimulación tales como la nano-cirugía. Este sistema fue desarrollado de tal manera que permite realizar microscopía confocal o de multifotón tanto de manera independiente como simultónea.

Así, la estación de trabajo permite realizar microscopía confocal de fluorescencia, microscopía de barrido láser de campo brillante y microscopía mediante la técnica de generacin de segundo harmónico (SHG), todos de manera simultánea. Las componentes de microscopía no lineal se han añadido al microscopio confocal explotando la gran versatilidad del mismo y sin tener que realizar ninguna modificación mecánica o electrónica al microscopio confocal.

La estación de trabajo multimodal fue utilizada para observar, mediante varias de las técnicas de microscopía incorporadas, los efectos de nano-cirugía y sus dinámicas asociadas. Así, un gran número de efectos, tales como derramamiento de axoplasma o la contracción muscular inducida por los pulsos láser, fueron observados con el microscopio, además de permitir la visualización de una gran cantidad de daños colaterales. Todos estos efectos estan reportados en este trabajo. Cabe mencionar que esta nueva herramienta para caracterizar daño colateral es superior a las técnicas establecidas para ello. Finalmente, la microscopía mediante SHG ha sido introducida como una nueva técnica para detectar daño colateral a los músculos que rodean las neuronas a las cuales se les practicú la nano-cirugía.

Thesis Publications

1. **Manoj Mathew**, Susana I.C.O Santos and Pablo Loza-Alvarez, "Femtosecond laser axotomy of D-type motoneurons and muscle damage assessment with Second Harmonic Generation (SHG) microscopy in *Caenorhabditis elegans*" Submitted to *J. Biomed. Opt.*

2. **Manoj Mathew**, Susana I.C.O Santos and Pablo Loza-Alvarez, "Real time imaging of femtosecond laser induced nano-neurosurgery dynamics in *C. elegans*" Submitted to *Opt. Exp.*

3. **Manoj Mathew**, Ivan Amat-Roldan, Rosa Andrés, Susana I. C. O. Santos, David Artigas, Eduardo Soriano and Pablo Loza-Alvarez, "Signaling effect of NIR Pulsed Lasers on Axonal growth" Submitted to *J. Neurosci. Meth.*

4. **Manoj Mathew**, Susana I.C.O Santos and Pablo Loza-Alvarez, "Multimodal optical workstation for simultaneous linear, nonlinear microscopy and nanomanipulation: Upgrading a commercial confocal inverted microscope" *Rev. Sci. Instrum.* **80**, 073701–073711 (2009)

5. **Manoj Mathew**, Ivan Amat-Roldan, Rosa Andrés, Iain. G. Cormark, David Artigas, Eduardo Soriano and Pablo Loza-Alvarez, "Influence of distant femtosecond laser pulses on growth cone filopodia" *Cytotechnology* **58**, 103–111 (2008)

Contents

Chapter 1

Introduction

1.1 Neurophotonics

In recent years light has emerged as a very powerful tool in the biomedical field for investigation, diagnosis as well as therapies. The works described in this thesis aim to extend these efforts into the fields of neurobiology and medical neurology, in a field that we have loved to call *Neurophotonics*. Neurophotonics aims to use the science and technology of photonics in neuroscience and has enormous potential to unravel the many mysteries that still surround neuorscience, in addition to providing new therapeutics to the neurosurgeon. In short this field aims to use light as a tool on neurons and the nervous system. The possible directions in which this field can lead us is immense, however in this thesis we have focused our attention mainly on two important aspects:

1. Using light as a tool to guide the growth of axons of neurons *in-vitro*.

2. Using light as a tool to perform subcellular neurosurgery and observe its dynamics *in-vivo* in the model organism *C.elegans*.

Such studies assume significance mainly due to two reasons. Firstly from an applied point of view, there are many medical conditions like spinal cord injury for which a robust treatment is still elusive. 300,000 estimated new cases of spinal cord injuries are reported worldwide every year. Current techniques offer only limited medical intervention and a majority of the patients live with life long paralysis or succumb to their injuries. A proper treatment calls for reconnecting back the broken circuit with precise control at the cellular level. Medical science is currently hunting for tools to help tackle this problem. A possible methodology for a robust therapy involves developing tools to image with high resolution the damaged neurons *in-vivo*, tools to induce precise incisions at the subcellular level to trim of edges of damaged regions and finally tools that could induce growth in the severed axons and guide them to their targets. Recent evidences suggest that light could very well be the tool we are searching for.

Secondly from the point of view of fundamental neuroscience there are many questions that have not been fully understood. One of them is neuron guidance. A large number of biochemical guidance cues have been identified and their functions in neuron guidance elucidated. However it is still not exactly clear how the extremely complex neuronal circuit

gets wired up during development. Many links seem to be missing. Light might be one such missing link. Indications that neurons could detect and respond to light sources could provide an entirely new dimension to the understanding of neuron guidance. In addition there also seems to be a lack of understanding in what goes on when axons get severed and what mechanisms govern their regrowth and reconnection. Optical tools that can target individual axons and sever them with minimal collateral damage could provide new insights into these questions as well.

1.2 Outline of this thesis

The works described in this thesis can be divided primarily into the following four sections,

1. **Optical Neuron Guidance**: Exploring the ability of NIR light to act as a signaling agent and to influence the behavior of growth cones and the trajectory of axons, in neurons from embryonic mouse cerebral cortex, *in-vitro*.

2. **Multimodal Optical Workstation**: Development of a novel imaging tool, build around a commercial confocal microscope that enables simultaneous linear and non-linear/multiphoton imaging and nano-manipulation.

3. **Nano – Neurosurgery**: Using the developed multimodal optical workstation to perform subcellular neurosurgery and observe its dynamics *in-vivo* and detecting collateral damage, while preforming surgery, using novel imaging tools like SHG imaging, in the model organism *C.elegans*.

4. **Genetic Cloning**: Using molecular biology tools to clone genes, mutations in which lead to a twisted pharynx phenotype in *C.elegans*.

1.2.1 Optical Neuron Guidance

One of the standing goals of neuroscience is to look for ways to control neuron/axon growth. Growing axons have a highly motile structure called the growth cone. During development the growth cone follows a precise pathway towards its target by scanning the extra-cellular matrix using the filopodia. Growth cone receptors sense external cues (biomolecules) that ultimately guide axons towards the correct target. In the last twenty years there have been significant efforts in finding alternative guidance cues (other than biomolecules) that can manipulate and enhance the intrinsic natural growth process. Several methods have thus been suggested including the use of electric fields, use of micropatterned substrate structures to restrict axonal growth to specified trajectories and mechanical forces.

A number of works also have highlighted the use of light as a potential tool to achieve control on axon guidance. For example laser photolysis of caged Ca^{2+} ions was used to induce a tropic turning of the axon. Lights ability to impart mechanical forces has also been explored to achieve axon guidance in different cell lines. In these experiments a near infra-red continuous wave (CW) laser beam was made to fall on the edge of the growth cone to optically drag the neuron towards a certain course, using an optical tweezer like approach.

There had however not been any significant efforts to explore if light could act as a signaling agent for neurons. In other words if neurons could detect and respond to the presence of optical signals. Such an investigation seemed very meaningful since some similar effects had been reported before on other cell types. 3T3 cells for example were shown to extend pseudopodia towards single microscopic infrared light sources at a distance. These and other indications prompted us to explore the possible signaling mechanism of light and its use to control the growth process of axons.

For this a NIR laser beam was focused at some distance away from the growth cone of primary neuron cultures. Our initial studies on the filopodia pointed to their ability to orient themselves towards the direction of the laser spot placed at a distance from the growth cone only when femtosecond-pulsed regime was used. We subsequently explored how this initial influence of the distantly placed light on the filopodia translated onto the axon and modified its subsequent growth. Particularly axons ability to grow towards distantly placed NIR laser spots was investigated under different temporal regimes: continuous wave (CW), chopped CW and femtosecond (FS) pulses. We observed significant axonal growth towards the laser spot equally in FS and chopped CW regimes. This steering effect on the axon, however, was not well evident when CW laser light (without pulsing) was utilized.

These results, obtained using primary neuronal cell cultures, represent what we believe is an interesting discovery demonstrating the ability of axons' trajectories to be controlled remotely by the use of pulsating light sources. The fact that the beam spot is located at some distance from the axonal growth cone reduces any eventual photodamage. In the long term, this optically-based method has the potential to open up new alternatives in the search of effective therapies for neural and brain repair.

1.2.2 Multimodal Optical Workstation

The work on optical neuron guidance had shown the potential use of light to signal the growth cones of primary neuronal cells in cultures *in-vitro*. Now two important tasks were at hand. Firstly to discover the reasons behind this effect and secondly to achieve such effects *in-vivo* in a modal organism like *C.elegans*. In addition it was also aimed to achieve other neuro-manipulation effects like for example nano-surgery of axons i.e. to induce precise incisions with submicrometer accuracy *in-vivo* and study the induced effects. However we faced a major technical hurdle. Our optical system (nonlinear microscope) could at a time be used either to induce an effect (stimulation/manipulation) or to produce laser scanning images, but not both at the same time. This ability was important if we were to proceed towards achieving each of the two goals. For example if we were induce nano-neurosurgery in *C.elegans* it is important to be able to see the fluorescently tagged neurons using confocal microscopy or epi-fluorescence microscopy while the femtosecond laser beam is set to induce the surgical process. Hence we embarked on building the multimodal optical workstation, in which a multiphoton microscope with the ability to perform Two Photon Excited Fluorescence (TPEF) microscopy, Second Harmonic Generation (SHG) microscopy and Femtosecond Laser Induced Nanosurgery was build around a commercial confocal microscope where both the subsystems (confocal and multiphoton) could work independently and simultaneously.

The confocal microscope, ever since its introduction, has emerged as a very powerful and indispensable tool for biological imaging. Its ability to provide excellent axial resolution, collect 3D images of thick fluorescently labeled specimens, together with the user

friendliness and versatility of modern day commercial confocal microscopes, has made it the biologists preferred imaging tool. Nonlinear/Multiphoton microscopy techniques like, Two Photon Excited Fluorescence (TPEF) microscopy aim to overcome many inherent problems of linear fluorescence microscopy like enhanced photobleaching and low depth of penetration partly by the use of Near Infrared (NIR) light for excitation. Harmonic Generation microscopy [Second Harmonic Generation (SHG) and Third Harmonic Generation (THG) microscopy], goes a step further by providing intrinsic contrast (without need for labeling and thus not causing any photobleaching) and structural information below the resolution limit of light.

Multiphoton microscopes are starting to be fully commercialized. The most currently existing systems are home built. Since multiphoton and confocal microscopes share a very similar scanning and detection platform, a number of attempts have been made to convert commercial confocal systems into tools for nonlinear microscopy. Most of these works have attempted to route the ultrashort NIR light for nonlinear microscopy through the confocal scan head. This configuration has, however, two distinct drawbacks: 1) The confocal scan and detection heads have to be opened and modified to enable it to switch between confocal and multiphoton modes and 2) The microscope can, at a time, work either as a confocal microscope or as a nonlinear microscope, but not both simultaneously.

A tool that would allow full use of the advantages of both a multiphoton and a commercial confocal microscope, in such a way that both systems could work simultaneously, was, however, lacking. The developed multimodal optical workstation aims to address this issue. In this work we build, for the first time to our knowledge, a nonlinear/multiphoton microscope having a commercial confocal microscope as base (inverted Nikon C1-Si) in a way that both the confocal and multiphoton sections can work independently and simultaneously. This is done without tampering with any of the confocal microscope system (like the scan and detection heads). We fully exploit all the flexibility, offered by the commercial confocal system (such as: two filter turrets, four detection ports, DIC condenser and diascopic detector) and add: 1) a separate scan head, 2) separate detection systems, both in the forward and backward directions and 3) separate control systems and software. All these features are achieved without the need to alter any of the C1-Si microscope components.

The multimodal workstation has the following capabilities:

1. Simultaneous LSBF, SHG and TPEF imaging
2. Simultaneous Confocal, LSBF and SHG imaging
3. Simultaneous Epi-fluorescence, LSBF and SHG imaging
4. Simultaneous Confocal imaging, Brightfield imaging and Femtosecond laser induced stimulation/manipulation
5. Simultaneous Epi-fluorescence imaging and Femtosecond laser induced stimulation/manipulation

1.2.3 Nano-Neurosurgery

Light can be used as a powerful tool for biological and medical applications. Short pulsed lasers have been used for more than 20 years in the manipulation and disruption

of transparent materials, including biological materials. Femtosecond laser ablation has significant advantages since it allows confinement of the induced incision primarily to the focal volume (< 1 femtoliter) of the tightly focused laser beam, owing to the involvement of nonlinear mechanisms in the ablation process. The femtosecond laser ablation tool is very powerful in performing Nano-neurosurgery, which helps in the better understanding of neuronal growth and regeneration.

Nano-neurosurgery was first performed by an American group in the model organism *C.elegans*. In this study individual D-type motorneurons were precisely cut with focused amplified KHz repetition rate, femtosecond laser pulses inside the anesthetized worm inducing a behavioral response (after surgery the worms were not able to move backwards; the shrinker phenotype). Within 24 hours most of the targeted neurons regrew and restored their function which allowed the worms to regain their characteristic body movement. This was a major technical and scientific advancement. Even though neuron regeneration was known for a long time, this was the first time it was demonstrated *in-vivo* in a single neuron. Many similar works were reported later.

Most of these works used brightfield or epi-fluorescence microscopy for observation of the dynamics of the process of Nano-neurosurgery and to detect possible collateral damage. These imaging tools by themselves however donot give enough details, which are significant in understanding the process of nanosurgery as such and the collateral damage induced to surrounding structures. This work addresses this issue. In this study we demonstrate various imaging techniques, to assist in the study of the laser nanosurgery and its dynamics, using the multimodal optical workstation. These imaging techniques, which are provided in a single mutimodal optical workstation, can be used for real-time imaging as well as immediate post-surgical determination of the efficiency of the process. With this tool several dynamic phenomena concomitant with laser nanosurgery in *C. elegans* were observed and imaged. Some of these dynamic phenomena, like muscular contraction, have been imaged for the first time during nano-neurosurgery of *C.elegans*.

In all studies so far the assessment of the cut/damaged area was done by visual examination of the post surgical images or by physical (theoretical) determination of the affected volume considering the characteristics of the laser. In this work the ability to simultaneously obtain high axial resolution confocal microscopy and brightfield images while performing axotomy provides the ability to observe the process of axotomy and the dynamics happening in the surrounding structures during this process. This in addition to providing a better insight into the the various dynamics happening during the course of nanosurgery, helps detect possible collateral damage. Moreover, we present a promising damage assessment technique to determine minute damages in nearby tissues such as muscle. We propose the use of Second Harmonic Generation (SHG) microscopy performed post-surgically as a means to detect the presence of damage if any to the muscles surrounding the axons as a result of the axotomy procedure.

1.2.4 Genetic Cloning

The works described in this thesis, so far, has involved the use of optical tools to induce axon guidance and cell manipulation in neurons, as well as development of multimodal microscopy tools to study various biological structures. However some important questions like why axons respond to distantly placed light sources requires a better understanding of biology and biological tools, particularly molecular biology and genetics. With this idea

in mind I spent five months in the group of Dr. Marc Pilon, in the department of cell and molecular biology in Gothenburg University, Sweden and participated in a project that involved cloning of certain genes, mutations in which cause the twisted pharynx phenotype.

The pharynx is a prominent feature in the head of *C.elegans* that pumps rhythmically to suck bacteria into the lumen and grind them for digestion. Several *C.elegans* mutants show the twisted pharynx phenotype. The *mnm-4(et4)* mutant was isolated in a screen for abnormal morphology of the M2 pharyngeal neurons. The M2 neurons showed a twisted phenotype which was subsequently attributed to an overall twist in the whole pharynx. A similar observation was made in screen for abnormal amphid sensory neuron dendrites. The mutant *sa580* showed twisted amphid sensory neuron dendrites, again due to an overall twist in the pharynx.

A set of molecular biology protocols were performed to identify the genes responsible for the twisted pharynx phenotype and location of the mutation in the genes. The protocols involved cloning of fragments of a gene that was a possible candidate of the mutation into a plasmid vector and subsequent sequencing of the recombinant plasmid DNA. The mutation responsible for both twisted pharynx phenotype in both the strains *mnm-4(et4)* and *sa580* was located in the *mig-6* gene. This gene codes for an extracellular matrix protein papilin.

1.3 Chapters in this thesis

This thesis is divided into nine chapters. The first four chapters give a general introduction to the concepts required to understand the works described in this thesis, the next four chapters describe the research done including the tools developed to carry out the research and the final chapter gives the a short conclusion and overview of possible future works. An appendix has also been included with details that are not directly relevant in understanding the thesis like biological preparatory protocols.

1.3.1 Chapter 2: Optical Tools in Biology

This chapter gives a general overview of the optical tools used in biology. Emphasis has been placed on the tools that were used as part of research described further in this thesis. The optical tools have been divided into linear and non-linear ones. The linear tools use single photon principles and have been used by biologists for a long time and are well commercialized. Principles of brightfield microscopy, DIC microscopy, fluorescence microscopy and confocal microscopy have been described. Nonlinear tools have been developed in the last decade or so and have provided many advancements in the understanding of biological processes. Two Photon Excited Fluorescence (TPEF) Microscopy, Second Harmonic Generation (SHG) microscopy and Femtosecond Laser Induced Nanosurgery are described.

1.3.2 Chapter 3: Neuron Guidance

One of the main themes of this thesis is achievement of neuronal guidance using light. Neuron guidance is one of the important aspects of neuroscience. During development of the nervous system, neurons project axons over long distances in order to reach their final targets. Along the way, growth cones located at the leading edges of axons detect and respond to environmental cues that guide them to their appropriate targets. These guidance cues, both attractants and repellents, include contact-mediated or secreted molecules,

acting over short or long distances, respectively. Axon guidance can be considered as the process of favored axon outgrowth towards or away from a particular region. Thus, axon guidance can be thought of as a process of biasing the extension/retraction of one side of the growth cone or axon shaft, compared to the other side. This chapter discusses the structure of growth cones, the chemical basis of neuron guidance, various methods to externally induce neuron guidance and finally optical tools used in neuron guidance.

1.3.3 Chapter 4: Biological Samples

This chapter discusses the biological samples used in experiments described in this thesis and their culture methods. For the first series of experiments neurons form cerebral cortex of mouse embryos were used. The initial part of this chapter hence describes basic cell culture methods and subsequently protocols involved in culturing neuronal cells form mouse embryos. The later experiments described in this thesis use the model organism *C.elegans*. The later part of this chapter describes the basic biology of *C.elegans* and also looks into the muscular and nervous systems of this model organism. The final part of the chapter describes the *C.elegans* culture methods.

1.3.4 Chapter 5: Optical Neuron Guidance

One of the standing goals of neuroscience is to look for ways to control neuron/axon growth. To externally induce guidance, several techniques have been employed including electric fields and use of focused light as optical tweezers. Ideally a mechanism that closely resembles the natural process of signaling the growth cone is desirable. Light can act as as putative agent to signal the growth cones and hence direct axonal growth. One of the primary aims of this thesis has been this study on the possible use of light to signal the growth cone in neurons. This chapter first describes, short duration observations of the filopodia, under the influence of weak NIR light sources. These light sources were placed close to the growth cone but not touching them. Filopodia are the fundamental path finders in the growth cone of the developing neuron. Once it was established that the filopodia significantly orient themselves towards light of certain properties, long duration observations were made to study the effect of these distantly placed light sources on the whole axon. It was observed that the initial orientation of the filopodia subsequently leads to the whole axon growing towards the laser spot in a statistically significant number of cases if pulsed NIR laser light is used.

1.3.5 Chapter 6: Multimodal Optical Workstation

In this work we propose and build a multimodal optical workstation that extends a commercially available confocal microscope (Nikon Confocal C1-Si) to include nonlinear/multiphoton microscopy and optical manipulation/stimulation tools such as nanosurgery. The setup allows both subsystems (confocal and nonlinear) to work independently and simultaneously. The workstation enables, for instance, nanosurgery along with simultaneous confocal and brightfield imaging. The nonlinear microscopy capabilities are added around the commercial confocal microscope by exploiting all the flexibility offered by this microscope and without need for any mechanical or electronic modification of the confocal microscope systems. As an example, the standard differential interference contrast condenser and diascopic detector in the confocal microscope are readily used as a forward detection mount for second harmonic generation imaging. The various capabilities of this

workstation, as applied directly to biology, are demonstrated using the model organism *C.elegans*.

1.3.6 Chapter 7: Nano-neurosurgery

The use of laser as a scalpel in both medicine and biology is starting to be widespread with several different applications. Femtosecond laser axotomy has proven to be a powerful tool for the study of subcellular phenomena especially, neuron regeneration in the earthworm *Caenorhabditis elegans*. The axotomy is an active process that lasts for a very short duration of time and that can (depending on the circumstances) lead to varying degree of collateral damage. Currently, real time imaging of the cutting procedure is limited to linear fluorescent techniques. This chapter describes various choices of imaging techniques, both linear and nonlinear, to assist in the study of the dynamics of the process of laser Nano-neurosurgery. Moreover, in addition to real time imaging and damage assessment in neighboring tissues (with the currently used DIC or epi-fluorescence and confocal imaging), this chapter describes an original technique to determine minute damages in close by tissues such as muscle. We propose the use of Second Harmonic Generation (SHG) microscopy as a novel tool to assess collateral damage. These studies put forward novel uses of the multimodal optical workstation setup that allows simultaneous imaging, by both linear and non-linear imaging modalities, and cell manipulation.

1.3.7 Chapter 8: Cloning *mnm-4(et4)* and *sa580* Genes in *C. elegans*

The works described in this thesis, until the previous chapters have involved the use of optical tools to induce axon guidance and cell manipulation in neurons, as well as development of multimodal microscopy tools to study various biological structures. However some important questions like why axons respond to distantly placed light sources requires a better understanding of biology and biological tools, particularly molecular biology and genetics. With this idea in mind I spent five months in the group of Dr. Marc Pilon, in the department of cell and molecular biology in Gothenburg University, Sweden. This chapter describes my efforts at the Gothenburg University, in cloning the gene in *mnm-4(et4)* and *sa580* causing the twisted pharynx phenotype and some studies related to their functions.

1.3.8 Chapter 9: Conclusion and Future Prospects

This chapter provides some general conclusions that can be drawn from the research described in this thesis and also looks into the future prospects.

Chapter 2

Optical Tools in Biology

2.1 Overview

Light was the first tool that helped biologists look closely at the biological world. Optics in the form of the microscope revealed the basic units of life. The simple optical microscope was invented in 1595 and more than 400 years on, it is still one of the most powerful tools to study biology. Microscopy has evolved into various powerful forms and together with many other new optical tools developed basically in the last century, plays a very significant role in biological investigations.

The various optical microscopic techniques used today include Bright-Field microscopy, Phase-Contrast microscopy, Nomarski(DIC) microscopy, Fluorescence microscopy, Confocal microscopy, Optical Coherence Tomography (OCT), Total Internal Reflection Fluorescence (TIRF) Microscopy, Stimulated Emission Depletion (STED) Microscopy, 4π microscopy and so on. Non linear optics has also come into the foray providing some great techniques like Two Photon Excited Fluorescence (TPEF) microscopy, Second Harmonic Generation (SHG) microscopy, Third Harmonic Generation (THG) microscopy, Coherent Anti-stokes Raman Scattering(CARS) microscopy etc:. In addition to all these far field techniques there has also been use of near field optics for microscopy namely Near Field Scanning Optical Microscopy (NSOM). Only a few important ones have been named here; many more optical microscopic techniques are in use.

In addition to microscopy light has provided many more tools to aid the biologists, like spectroscopy, optical tweezers, optical sensors, optical scalpel for surgery and photodynamic therapy, to name a few.

As can be seen there are numerous tools provided by optics in biology and medicine. This chapter discusses briefly only those techniques that were used in the research described in the later chapters.

2.2 Linear Techniques

2.2.1 Optical Microscopy

In simple terms the optical microscope is a device that uses light and combination of lenses to produce a magnified image of objects not easily seen by the naked human eye.

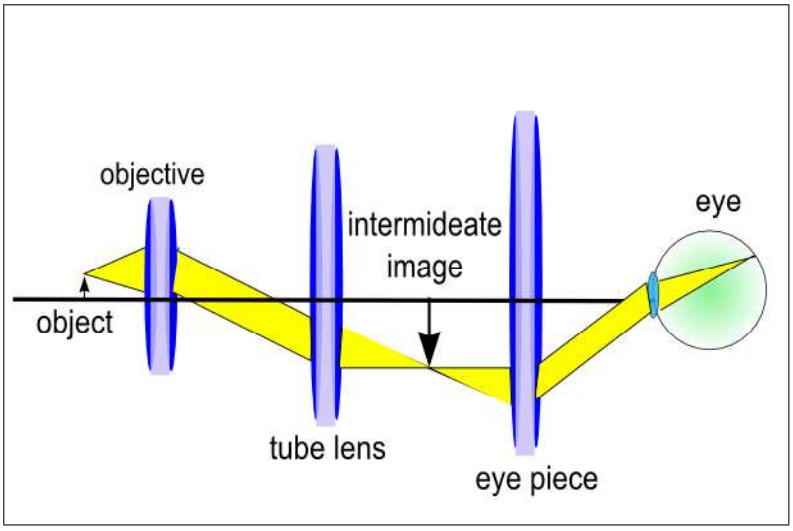

Figure 2.1: Optical train of the infinity-corrected microscope system

Modern microscopes provide magnified two dimensional images together with the ability to obtain them form successive focal planes, hence providing two and three dimensional visual information of the fine structure of the sample under observation.

The microscope optics basically consists of an illuminator (including the light source and collector lens), a condenser, specimen, objective, eyepiece, and detector. Most modern microscopes employ the Köhler illumination arrangement in which the collector lens and other optical components project, an enlarged and focused image of the lamp filament onto the plane of the aperture diaphragm of a properly positioned condenser. The condenser concentrates this light in the form of collimated beam pencils, into a cone of light that illuminates the specimen with these beams of uniform intensity from all azimuths over the entire viewfield. The light source is not focused onto the specimen, hence the illumination at specimen is very much grainless and extended, and does not suffer distortion.

The objective lens is like a magnifying glass with very high magnification i.e. a lens with a very short focal length, which is brought close to the sample plane. The light form the sample plane is focused by the objective to a point inside the microscope tube. This real and inverted image is viewed by the eyepiece lens that provides further magnification. Most modern microscopes are infinity corrected; ie. sample is placed at the objective back focal plane and the objective produces a collimated beam of light that propagates into the microscope tube. This beam is brought to focus by the tube lens. The tube lens hence forms an intermediate image in the back focal plane of the eye piece. The total magnification of the microscope is equal to the magnification by the objective times that of the eyepiece. There is essentially an infinity space that is defined by parallel light beams in every azimuth between the objective and the tube lens. This space is used in the microscope to add accessories such as vertical illuminators, differential interference contrast (DIC) prisms, polarizers, epi-fluorescence illuminators etc:. Figure 2.1 illustrates the optical train using ray traces of an infinity-corrected microscope system.

Microscope specimens can be considered as complex gratings with details and openings of various sizes; a concept developed by the famous German microscopist and optics the-

oretician Ernst Abbe. The details of a specimen will be resolved if the objective captures the 0th order of the light and at least the 1st order (or any two orders, for that matter). The greater the number of diffracted orders that gain admittance to the objective, the more accurately the image will represent the original object [1–3]. Further, if a medium of higher refractive index than air (such as immersion oil) is used in the space between the front lens of the objective and the top of the cover slip, the angle of the diffracted orders is reduced and the fans of diffracted light will be compressed. As a result, an oil immersion objective can capture more diffracted orders and yield better resolution than a dry objective. Moreover, because blue light is diffracted at a lesser angle than green light or red light, a lens of a given aperture may capture more orders of light when the wavelengths are in the blue region of the visible light spectrum. These two principles define the classic Rayleigh principle [1; 3–5] described by the equation

$$d = \frac{1.22 \times \lambda}{2 \times (N.A_0 + N.A_c)} \tag{2.1}$$

where d is the smallest distance between two points that can be resolved, λ is the wavelength of illumination light, N.A$_o$ is the numerical aperture of the objective and N.A$_c$ is the numerical aperture of the condenser.

2.2.2 DIC Microscopy

DIC microscopy is one of the techniques that enables visualization of phase objects [6]. Phase objects donot absorb light and hence are difficult to observe under normal bright field illumination. However they alter the phase of the light because of a refractive index change.

The optical components specific to the DIC microscope are the linear polarizer (inserted between the light source and the condenser), a modified Wollaston prism (mounted close to the iris in the condenser back focal plane), a Nomarski prism (inserted immediately behind the objective) and an analyzer (mounted before the tube lens and the image plane. The polarizer and analyzer are crossed. The prisms are each made by joining two thin crystal optical wedges whose optical axis are perpendicular to each other. A different prism is needed for each objective of different magnification. A beam of light entering normal to one face of the prism would be split into the orthogonal s and p polarizations. Without the prisms the DIC microscope would work as a polarized light microscope tuned to work at maximum extinction.

In a typical DIC microscope the polarizer is set to pass the p polarized light which is split equally into s and p polarizations at the modified Wolloston prism with its shear axis at 45^0 to the beam. These two rays travel close together but in slightly different directions (illustrated in Figure 2.2). The rays intersect at the front focal plane of the condenser, where the lens converts the small angular deviation in the s and p polarizations into a fixed transverse spatial offset. The rays hence pass traveling parallel and extremely close together with a slight path difference, but since they are orthogonal are unable to cause interference. The distance between the rays, called the shear, is so minute that it is less than the resolving ability of the objective.

The split beams enter and pass through the specimen where their wave paths are altered in accordance with the specimens varying thickness, slopes, and refractive indices. These variations cause alterations in the wave path of both beams passing through areas

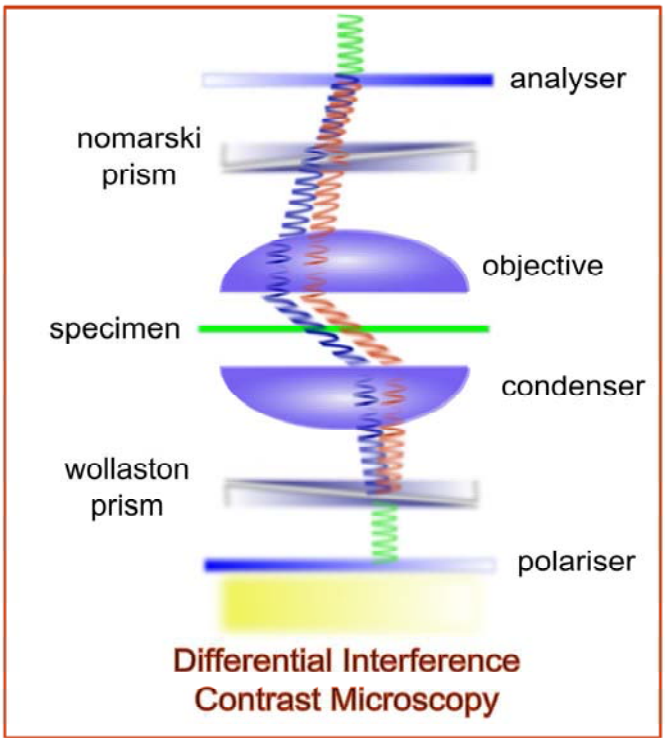

Figure 2.2: Schematic illustration of microscope configuration for differential interference contrast (DIC) (red and blue light paths represent s and p polarizations respectively)

of the specimen details lying close together, inducing phase delays. When the parallel beams enter the objective, it reconverts the spatial offset of the s and p back into angular divergence. An inverted Wolloston prism ideally would converge these diverging beams if kept at the back focal plane of the objective but unfortunately many objectives donot allow much room for this at its back focal plane [7]. Nomarski solved this problem by modifying the Wolloston prism so that it could be located immediately behind the objective. Such a prism is called the Nomarski prism and recombines the diverging s and p fields, thus removing the shear.

The phase gradients impressed on the offset s and p fields in passage though the specimen are therefore converted into phase differences, creating elliptical polarization in the recombined field [7]. In order for the beams to interfere, the vibrations of the beams of different path length must be brought into the same plane and axis. This is accomplished by placing a second polarizer (analyzer) after the Nomarski prism. The Nomarski prism exactly compensates for the effect of the modified Wolloston prism and the analyzer extinguishes the light in the locations where there is no phase gradient. The light then proceeds toward the eyepiece where it can be observed as differences in intensity and color [7]. The resulting image hence shows the refractive edges as bright features while the rest of background is dark. The effect of one side of a detail appearing bright (or possibly in color) while the other side appearing darker (or another color) provides a pseudo three-dimensional appearance to the specimen.

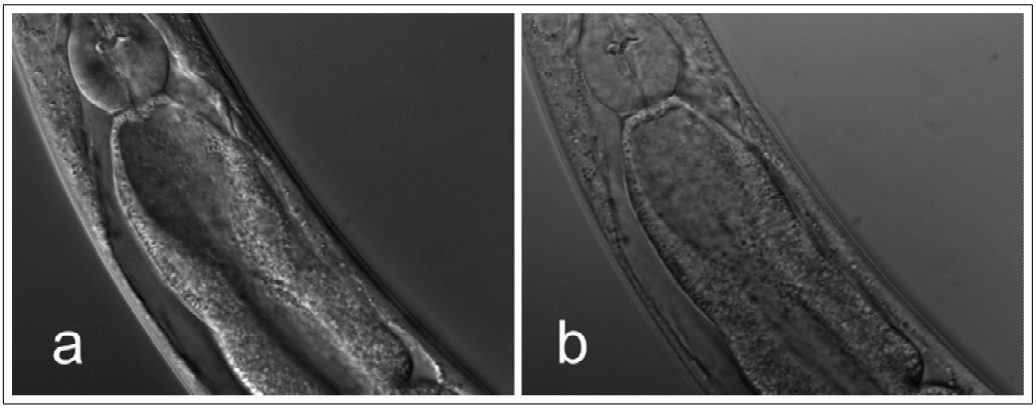

Figure 2.3: Comparison of *C.elegans* images a) with DIC optics and b) without DIC optics

Figure 2.3 shows the same image of an *C.elegans* worm acquired with and without DIC optics. It can easily be appreciated that the DIC optics provides a much better contrast.

2.2.3 Fluorescence Microscopy

Biological samples are quite complex structures and looking for something very specific in them (for example looking at neurons inside *C.elegans* larvae) could be almost impossible many a times. Fluorescence microscopy [8–10] comes in very handy in such a situation. Here a component of interest in the specimen is specifically labeled with a fluorescent molecule called a fluorophore (such as green fluorescent protein (GFP), fluorescein etc:). Then by observing the fluorescence of the label the component of interest can be observed. Figure 2.4 shows the schematic of a fluorescence microscope.

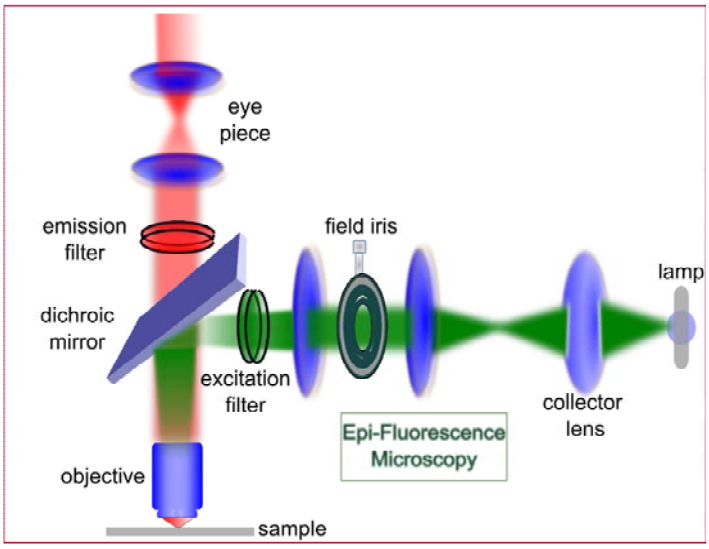

Figure 2.4: Schematic diagram of the configuration of fluorescence microscope. (green and red light paths represent excitation and emission respectively)

As shown in the Jablonski diagram (Figure 2.5) the excitation process usually brings

the fluorophore from its singlet electronic ground state to its lowest excited singlet sate. The vibrational broadening of this excited state leads to a band of wavelengths (absorption spectrum) with which the fluorophore can be excited. Vibrational relaxation of electronic states occurs rapidly causing the fluorophore to relax to the bottom of the excited state.

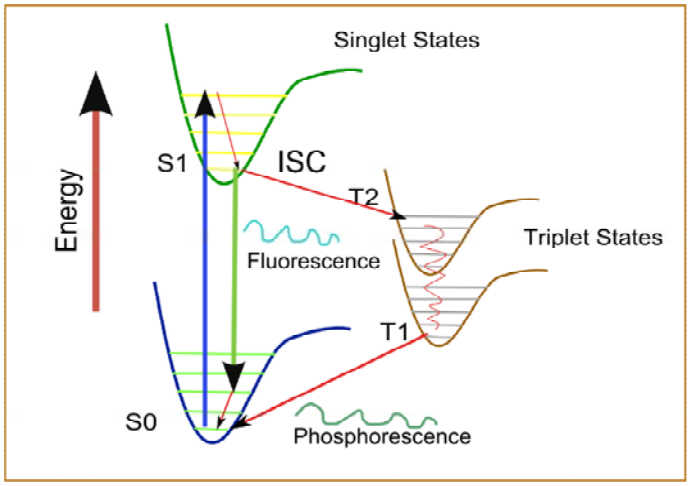

Figure 2.5: Jablonski diagram depicting fluorescence and phosphorescence

The lifetimes in the excited states are usually in the nanosecond timescale but are affected by the relative rates of non-radiative decay, spontaneous emission, stimulated emission, inter-system crossing, or quenching. Fluorescence is observed when a photon is emitted by the fluorophore as it returns directly to the ground state. There is an energy loss associated with the internal energy conversion, so fluorescence occurs at a lower photon energy compared to the excitation photon energy (stoke's shift). The return to the electronic ground state may leave the fluorophore transiently in a vibrationally excited state prior to rapid internal conversion to the lowest ground level. This allows for a range of emitted photon energies, observed as a fluorescence spectrum. When expressed on a quantum basis of photons fluoresed versus absorbed photons, the quantum yield is the fractional probability with which fluorescence will occur relative to other relaxation modes [7].

Spontaneous spin unparing of of two electrons in the excited state can occur due to molecular collisions. This process known as inter-system crossing (ISC), is enhanced by spin-orbit coupling [11; 12] when the dye contains one or more heavy atoms (Cl,Br,I). The resulting triplet state is reactive and highly susceptible to quenching due to its long intrinsic lifetime. If not quenched, a triplet can relax by phosphorescence (Figure 2.5) resulting in emission of photon at an energy lower than the fluorescence. In figure 2.5 T1 and T2 represent the triplet states. Triplets are very effectively quenched by dissolved molecular oxygen which is very prevalent, highly diffusible, and has a triplet state. Oxygen quenching of fluorophore triplets can produce oxygen singlets, a long lived excited state of O_2, or several forms of oxygen radical. Dye triplets can also react directly with other organic molecules, especially intracellular redox intermediates. As a result of this photochemistry photo-bleaching and photo-toxicity can occur [7].

In the most common optical configuration for fluorescence microscopy a broadband

light from an intense lamp is directed into the microscope through the excitation filter, which is chosen to match the excitation band of the fluorophore. The resulting filtered light is deflected by the matched dichroic reflector (Figure 2.4) into the back pupil of the objective. This forms an epi-fluorescence configuration, where the objective also functions as the condenser, in addition to its usual role. High NA objectives hence function as more powerful condensers and also collect a greater fraction of fluorescence emission light. The backscattered excitation light is reflected out by the dichroic. The fluorescence emission passes efficiently through the dichroic and through the emission filter which is usually a bandpass filter designed to efficiently transmit the fluorescence emission spectrum, and efficiently block all other light. This allows the fluorescence image to be formed in a dark background to give maximum sensitivity. The light out of the emission filter is focused to form an image.

2.2.4 Confocal Microscopy

In fluorescence microscopy, because a large volume is excited and samples often emit form the whole excited volume, images are often degraded by light that is scattered or emitted by structures outside the plane of focus. As a direct consequence, there is poor depth discrimination, or in other words very poor axial resolution [13]. This renders the fluorescence microscope inefficient for producing tomographic images of the sample. Tomographic imaging; that is the capturing images from consecutive focal planes, is very essential in localizing fluorescent targets in the three dimensional space. Confocal microscopy [14–20] provides high axial resolution and enables such tomographic imaging, very efficiently overcoming the drawbacks of the conventional fluorescence microscopic techniques.

The principles of confocal microscopy was developed by Marvin Minsky [21; 22] in the year 1961. The confocal optics projects an image of a focally illuminated point in the specimen onto a small aperture in the conjugate focal plane as shown in Figure 2.6. Fluorescent signal form the point where the excitation light is focused would pass through the pinhole onto the detector. Fluorescent signal from out of focus points would be spread out and be blocked by the pinhole. This gives the confocal microscope an edge with respect to the conventional optical microscopy in terms of controllable depth of field, the elimination of image degrading out-of-focus information, and the ability to collect serial optical sections from thick specimens [23–25].

Most of technicalities of the confocal microscope are built into its scan head. The scan head consists of inputs form external laser sources, fluorescence filter sets and dichromatic mirrors, a galvanometer-based raster scanning mirror system, variable pinhole apertures for generating the confocal image, and photomultiplier tube detectors tuned for different fluorescence wavelengths. Coherent light emitted by the laser system (excitation source) passes through a pinhole aperture which is situated in a conjugate plane (confocal) with respect to a scanning point on the specimen (see Figure 2.6) and a second pinhole aperture positioned in front of the photomultiplier tube detector.

The image of an extended specimen is generated by scanning a focused beam across a defined area [26; 27] in a raster pattern, controlled by two high-speed oscillating mirrors driven with galvanometer motors. These mirrors are mounted orthogonal to each other and their motors are controlled electronically.

The laser light is reflected by a dichromatic mirror, and focused onto the objective.

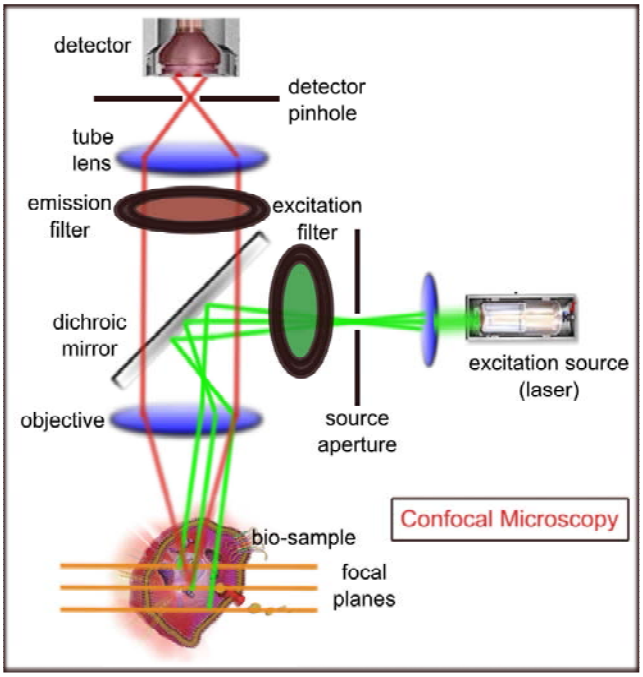

Figure 2.6: Schematic diagram of the configuration of confocal microscope. (green and red light paths represent excitation and emission respectively)

The confocal microscope works in the epi-illumination configuration. After expansion by a beam expander (to completely fill the objective numerical aperture), the excitation laser beam is focused to form an intense diffraction-limited spot that is scanned by the coupled galvanometer mirrors to produce the raster pattern across the specimen plane. This is much unlike the traditional widefield epi-fluorescence microscopy where the objectives collimate a wide cone of illumination.

The fluorescence emitted from points on the specimen (in the same focal plane) as a result of the raster scan is collected by the objective and passed back through the confocal optical system. The speed of the scanning mirrors is very slow relative to the speed of light, so the fluorescence emission follows a light path along the optical axis, that is identical to the original excitation beam. Return of fluorescence emission through the galvanometer mirror system is referred to as descanning [28; 29]. Such a descan is essential to direct the light onto the pinhole that is fixed irrespective of the spatial position of the point being excited.

The fluorescence emission which passes through the pinhole is made to pass through appropriate barrier filters and directed on to a Photo Multiplier Tube (PMT) detector. The PMT signal is sampled above the Nyquist rate by the detector electronics and an image is generated digitally. Once an image of a sample in a single focal plane is obtained, the focal point can be moved backward or forward to acquire another image in a different focal plane. This process can be repeated and a stack of images from consecutive focal planes can be obtained.

2.3 Nonlinear Techniques

All the techniques discussed until now in this chapter use effects where light interacts linearly with the sample. There are various microscopic techniques and other optical effects relevant to biology, where light is made to interact non linearly with the sample.

Light is said to interact nonlinearly with a material if it changes the optical properties of that material as it interacts. The field of non-linear optics [30–36] relates to study of all the effects resulting form such interactions. These effects arise essentially when very intense coherent optical radiation interacts with matter. Until the advent of such intense coherent optical sources, namely the laser, non-linear optics was a relatively unexplored field.

Nonlinear optical phenomena are 'nonlinear' in the sense that they occur when the response of a material system to an applied optical field depends in a nonlinear manner upon the strength of the optical field [30]. In linear optics the polarization $\tilde{P}$(t) (the dipole moment per unit volume) would depend linearly on the strength of the applied electric field $\tilde{E}$(t) and can be described by the equation:

$$\tilde{P}(t) = \chi^{(1)}\tilde{E}(t) \tag{2.2}$$

where $\chi^{(1)}$ is the linear susceptibility of the medium. By generalizing equation 2.2 and expressing the polarization $\tilde{P}$(t) as a power series, the optical response in the non-linear regime can be described as:

$$\begin{aligned} \tilde{P}(t) &= \epsilon_0[\chi^{(1)}\tilde{E}(t) + \chi^{(2)}\tilde{E}^2(t) + \chi^{(3)}\tilde{E}^3(t) + ...] \\ &\equiv \tilde{P}^{(1)}(t) + \tilde{P}^{(2)}(t) + \tilde{P}^{(3)}(t) \end{aligned} \tag{2.3}$$

The constant ϵ_0 is the permittivity of free space and constants $\chi^{(2)}$ and $\chi^{(3)}$ are called the second and third order susceptibilities respectively. Here the first term is the linear polarization and the rest are the nonlinear polarization terms (second order, third order and so on). The tilde over a quantity describes rapid variation of that quantity in time.

Time varying polarization gives rise to new components of electric field and hence polarization defined as a function of electric field (Equation 2.3) is used to describe non-linear optical phenomenon. If the excitation $\tilde{E}$(t) is small then the higher order terms are negligible and the medium does not exhibit much non-linear behavior. This is due to the fact that $\chi^{(2)} \approx \chi^{(1)}/E_{at}$, $\chi^{(2)} \approx \chi^{(3)}/E_{at}^2$ and so on, where E_{at} is the atomic electric field strength. Hence as the order of non-linearity increases the values of susceptibilities decrease exponentially. For the same reason exponentially increasing excitation field strengths are required to excite higher and higher orders of non-linearities. Fourier analysis of Equation 2.3 reveals that the polarization changes at frequencies that are higher order harmonics of the input optical excitation frequency [37]. This forms the basis of non-linear optics.

As described in the introduction of this chapter there are many non-linear optical techniques used in biology [18; 38–44]. These involve absorption or simultaneous interaction of more than one photons with the biological sample and hence are also called multiphoton techniques. Following sections describe four non-linear microscopic techniques namely Two Photon Excited Fluorescence (TPEF) Microscopy, Second Harmonic Generation (SHG) Microscopy, Third Harmonic Generation (THG) Microscopy and Coherent Antistokes Raman Scattering (CARS) Microscopy. In TPEF the non-linearity is in the absorption of

the excitation light and the emission is a linear process. In SHG and THG there is no absorption and the non-linearity is in the emission. The last section describes Ultrashort Laser Induced Nanosurgery, where the non-linearity is in the absorption.

2.3.1 Two Photon Excited Fluorescence (TPEF) Microscopy

The confocal microscope in the last decade or so has emerged as a very powerful optical imaging tool in the bio-medical field. Wide commercial availability coupled with versatility, user-friendliness and ability to perform multi-spectral excitation and multi-channel detection optical sectioning microscopy, has made it a gold standard in biological imaging. It however suffers from many drawbacks like:

1. Use of light in the blue end of the spectrum for excitation increases the possibility of phototoxicity and photobleaching. The danger of photobleaching is not confined just to the focal spot but also extends well above and below it.

2. Wavelengths in the blue especially, ultraviolet requires use of special optics amenable to them.

3. Since scattering is inversely proportional to the fourth power of wavelength, light in the blue end of the spectrum encounters increased scattering loses and does not penetrate deep into thick bio-samples. Hence imaging thick tissues is often a bottleneck.

4. Better axial resolution requires smaller pinholes resulting in low signal to noise ratio (SNR).

5. The excitation and emission spectra often are very close and sometimes even overlap, often making it difficult to separate the weak emission signal form the strong excitation.

Two-Photon Excited Fluorescence (TPEF) Microscopy [45; 46] in particular and multiphoton excitation microscopy in general provides a very different approach for optical section microscopy compared to confocal microscopy. This technique overcomes the problems of ultraviolet excitation and provides many new advantages of its own, but it requires other trade-offs [41].

Principles of Two Photon Excited Fluorescence

Two-photon excitation, paradoxically, excites fluorescence with photons of longer wavelength than the emitted light. Two photons of half the required energy arrive simultaneously and combine forces to excite the electron to the higher state. In most cases, the electron ends up in exactly the same (S1) excited state before it drops down to the ground state, so that the fluorescence emitted is identical to that given off by normal, single-photon excitation [41]. Figure 2.7 compares the process of single and two photon excitation.

The theory of Two Photon Excited Fluorescence was first described by Maria Göppert-Mayer [47; 48] in 1931. An important aspect of the Maria Göppert-Mayer's paper is that the process of two-photon absorption involves the interaction of two photons and an atom via an intermediate, "virtual" state [38]. This interaction must occur within the lifetime of this virtual or intermediate state. The virtual state can be described as a superposition

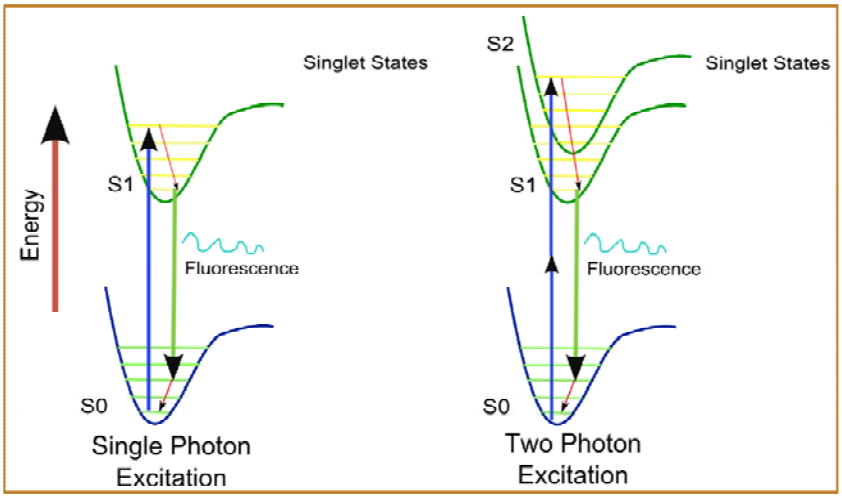

Figure 2.7: Jablonski diagram depicting the process of single photon and two photon excitation.

of states and is not a true eigenstate of the atom. The individual transitions (i.e., from the ground state to the virtual state, and a transition from the virtual state to the final state) each do not obey the law of conservation of energy; only the total transition, via two photons from the ground state to the virtual state and to the final state, obeys the law of conservation of energy [38]. The probability of the two-photon transition has contributions from all of the virtual intermediate states. The first photon induces the transition from the ground state to the virtual state, and the second photon induces the transition from the virtual state to the excited state. Both photons interact to induce the transition from the ground state to the excited state.

To have two photons arrive simultaneously at a single molecule requires a very large flux of photons impinging on the specimen. Excitation is therefore likely to occur only at the focus of the illuminating light, where the photon flux is very high. Above and below this point, the photons are not sufficiently concentrated, and two-photon events are vanishingly rare. The probability of two photons arriving at a point at the same moment depends on the probability of one photon being there multiplied by the probability of another photon being there [41]. In other words, it depends on the square of the flux density of photons. This means that as we move away form the focus since the intensity decreases almost quadratically and since the Two Photon Excited Fluorescence depends also quadratically on the intensity of excitation, the fluorescence diminishes almost to the fourth power of distance from the focal spot, making it vanishingly small at points away from the focus. This is very similar to what is obtained in a confocal microscope where the pinhole prevents out of focus light to be detected, but here with the advantage that the pinhole is not required. With no pinhole, only in-focus structures can be seen; optical sectioning in two photon microscopy is completely analogous to that in confocal microscopy [41].

A very high photon flux as required in two-photon microscopy requires a very high intensity on the focal plane typically of the order of around 1MW/cm^2 and would require a laser power of the order 1KW. This would almost completely damage the fragile biological

sample, if made to impinge on it. Moreover it would be almost prohibitive to manage such high power lasers for applications of microscopy. Since what damages is the energy and not the power, the trick used in multiphoton microscopy is to use ultrafast optical pulses usually in the femtosecond regime. Ultrafast optical pulses deliver small amounts of energy in extremely short amounts of time, hence delivering very large amounts of instantaneous power but with average powers comparable with that used in confocal microscopes. The ultrashort pulse durations are usually shorter than the thermal relaxation times of the bio-samples, which means that the pulse interacts for a time that it too short to heat the sample. It is very common to use modelocked Titanium Sapphire lasers for the purpose, which are tunable in the NIR and deliver typically with 100fs pulse widths and repetition rates of about 80-100MHz. The high repetition rate is advantageous to ensure that even with a fast scanning of the beam there are sufficient number of pulses interacting with each pixel, which when integrated over time gives a decent signal to noise ratio.

The Multiphoton Microscope

Multiphoton microscopes use the same principle for image generation as in confocal microscopes: laser scanning point by point image acquisition [26] and digital reconstruction of stored image data (see section 2.2.4). So in terms of construction the multiphoton microscope is quite similar to the confocal microscope with the exception that the pin hole is not required. A major advantage of multiphoton imaging is that scattered light that would not reach the pinhole in a confocal system can still be collected giving in principle an higher signal to noise ratio (SNR). Multiphoton microscopes are therefore equipped with non-descanned (i.e., wide-field) detectors. These can be placed either behind the objective, where the wide-field fluorescence illuminator would be, or beyond the condenser, where the transmitted illuminator would be. The choice of geometry is particularly relevant when second harmonic generation (SHG) microscopy (see section 2.3.2) also needs to be performed. This is because fluorescence is transmitted equally in all directions, but the second harmonic is preferentially transmitted in the forward direction.

Comparison of TPEF microscopy with confocal microscopy

Advantages

- Because two-photon events can take place only at the focus of the illuminating light, photobleaching above and below the plane of focus is eliminated.
- Penetration of the exciting light into tissue is increased by at least a factor of two due to its longer wavelength and lower Rayleigh scattering at these wavelengths.
- Because two-photon events occur only at the focus of the illuminating beam, there is no need for a confocal pinhole.
- The detection arrangement is much simpler since a non-descanned detection configuration can be implemented. Together with the fact that there is no need for the pinhole and the use of wide area detectors gives a better SNR.
- Long-wavelength light is much less damaging to living cells than ultraviolet or even blue light.

Disadvantages

- Very expensive and sophisticated laser systems are required.
- Use of higher wavelengths results in reduced lateral spatial resolution.
- The absence of pinhole, make multiphoton microscopes quite susceptible to ambient light. While in the confocal microscope the pinhole blocks most of the out of focus light and hence quite a bit of noise from the ambient light is tolerated.
- If imaging is performed on a single focal plane plane for long durations of time, the two-photon microscope would produce more photobleaching compared to confocal microscope.

2.3.2 Second Harmonic Generation (SHG) Microscopy

The Two Photon Excited Fluorescence microscopy overcomes a number of drawbacks of confocal microscopy however it suffers from the following fundamental problems of confocal microscopy in particular and fluorescence microscopy in general:

- Need for an endogenous or exogenous fluorophore.
- Use of fluorophores makes them susceptible to photo-bleaching and makes long duration imaging quite cumbersome.
- Since fluorescence is a non-parametric process only presence of the fluorophore is conveyed by fluorescence imaging and no additional information like orientation or organization of the structure of interest is revealed.

Imaging using parametric non-linear processes like Second Harmonic Generation (SHG) and Third Harmonic Generation (THG) overcomes to a great extend these drawbacks. This section only discusses SHG.

Principles of Second Harmonic Generation

Second Harmonic Generation (SHG) is the process in which light of wavelength ω after interaction with a material yields an output light of frequency exactly double the input ie. at 2ω (see Figure 2.8). The transfer of energy from the input field to the output field can be visualized in terms of the energy-level diagram shown on the right-hand side of the figure. In SHG as shown in Figure 2.8 two photons of frequency ω are destroyed and a photon of frequency 2ω is simultaneously created in a single quantum-mechanical process [30]. The solid line in the figure represents the atomic ground state, and the dashed lines represent the virtual levels. These levels are not energy eigen-levels of the free atom, but rather represent the combined energy of one of the energy eigenstates of the atom and of one or more photons of the radiation field. The process of second harmonic generation generalizes straightforwardly to direct third and higher-order harmonic generation [38].

As described before in equation 2.3 the study of nonlinear optical processes begin by considering how the response of the material medium, specified by means of the polarization P (dipole moment per unit volume), depends on the amplitude E of the electric field

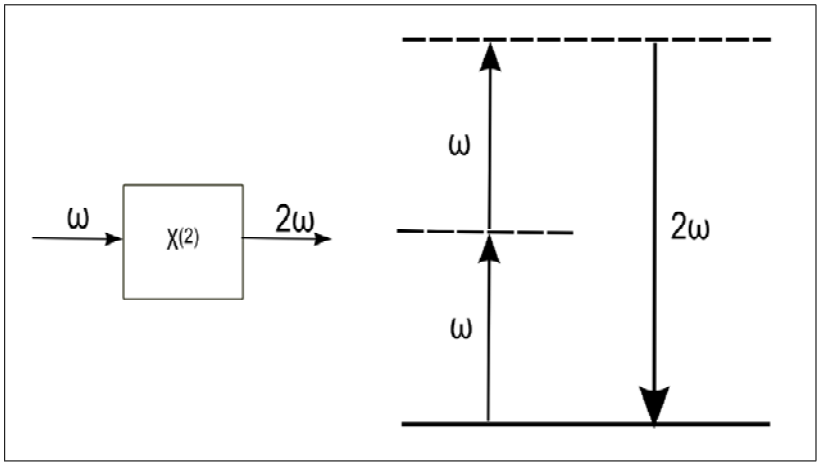

Figure 2.8: Diagram depicting the process of Second Harmonic Generation (SHG).

of the applied optical wave. If an electric field E is considered such that:

$$\tilde{E}(t) = Ee^{-i\omega t} + c.c \tag{2.4}$$

and if the second order susceptibility is non zero then from equation 2.3, the nonlinear polarization that is created in the crystal is given by [30]:

$$\begin{aligned} \tilde{P}^{(2)}(t) &= \epsilon_0 \chi^{(2)} \tilde{E}^2(t) \\ &\equiv 2\chi^{(2)} EE^* + (\chi^{(2)} E^2 e^{-i2\omega t} + c.c) \end{aligned} \tag{2.5}$$

It can be seen that the second-order polarization consists of a contribution at zero frequency (the first term) and a contribution at frequency 2ω (the second term). This latter contribution can lead to the generation of radiation at the second-harmonic frequency. The first contribution in equation 2.5 does not lead to the generation of electromagnetic radiation (because its second time derivative vanishes); it leads to a process known as optical rectification in which a static electric field is created within the nonlinear crystal [30].

The even order nonlinear susceptibilities vanish for a crystal with centrosymmetry. So second harmonic generation is restricted to those crystals which lack centrosymmetry. This is because the SHG wave is a vector quantity and the induced polarization in a centrosymmetric sample would be equal and opposite and vector adds up to zero [38]. As in two photon excitation, the amplitude of SHG depends on the square of the incident light intensity and since two photons need to arrive simultaneously, SHG requires a very large flux of photons impinging on the sample or in other words requires very high intensity excitation.

The second harmonic signal shows a strong tendency to propagate forward. The reason for the directionality lies in the coherent nature of the second harmonic generation process. The harmonic is always in phase with the exciting beam. Although an individual molecule will radiate the harmonic in all directions, as soon as there are several molecules within the excitation volume, the phase relationship among the individual radiators becomes important. The structural arrays oriented along the direction of the beam propagates

strongly forward; regardless of the actual spacing [41] . All dipoles have the same phase relationship to the exciting beam in the forward direction but are randomly out of phase in the reverse direction.

Use of SHG for microscopy

Many biological structures can be highly polarizable and can arrange into well ordered non-centrosymmetric structures making them excellent candidates for Second Harmonic Generation. Such structures are usually surrounded by others that lack these properties, making the use of second harmonic generation for microscopy [49] an excellent means to generate contrast with out need for fluorophores. SHG microscopy has been reported on collagen [50; 51], microtubules [52], muscle [53–55], starch [56] and cellulose [57].

The design of the SHG microscope is very similar to the TPEF microscope that is like a confocal microscope without a pinhole. Linearly excited\non-linearly excited fluorescence transmits equally well in the forward and backward direction. Hence confocal or TPEF microscopes can have the detector either in the forward or in the backward. However, it is much more convenient to have the detector in the backward since the same objective doubles as condenser for collection, saving equipment costs and alignment efforts. This however is not possible in a SHG microscope and it requires a forward detector, since SHG signal transmits preferentially in the forward direction. There are some materials like starch which gives a small amount of backward SHG apparently due to backscattering or non-complete destructive interference in the backward direction. This signal however is quite limited. Hence SHG microscopes do need a forward detection configuration. Figure 2.9 shows the schematic of a multiphoton microscope which can detect both in the forward and backward. This configuration can be used for simultaneous TPEF and SHG imaging. This configuration can also be used to detect Third Harmonic Generation (THG) instead of SHG by proper choice of filters and optics, since THG too propagates preferentially in the forward direction. Usually narrow band pass filters are utilized for SHG microscopy using the aforementioned multiphoton microscope configuration, so as to efficiently cut off the broad band signal arising form TPEF.

Comparison of SHG and TPEF Microscopy

Table 2.1 compares the techniques of Second Harmonic Generation (SHG) and Two Photon Excited Fluorescence (TPEF) [41]:

Table 2.1: Comparison between SHG and TPEF Microscopy

	(SHG)	(TPEF)
1	Exactly double excitation frequency	Less than double; by stokes shift
2	Largely frequency independent	Strongly frequency dependent
3	Virtually instantaneous: $\sim$ 1 fs	Lifetime in ns
4	Propagates essentially in the forward	Propagates in all directions
5	Coherent (in phase with exciting light)	Incoherent
6	No energy loss	Always energy loss
7	Requires short laser pulses	Requires short laser pulses
8	Requires no contrast generating agent	Requires fluorophore

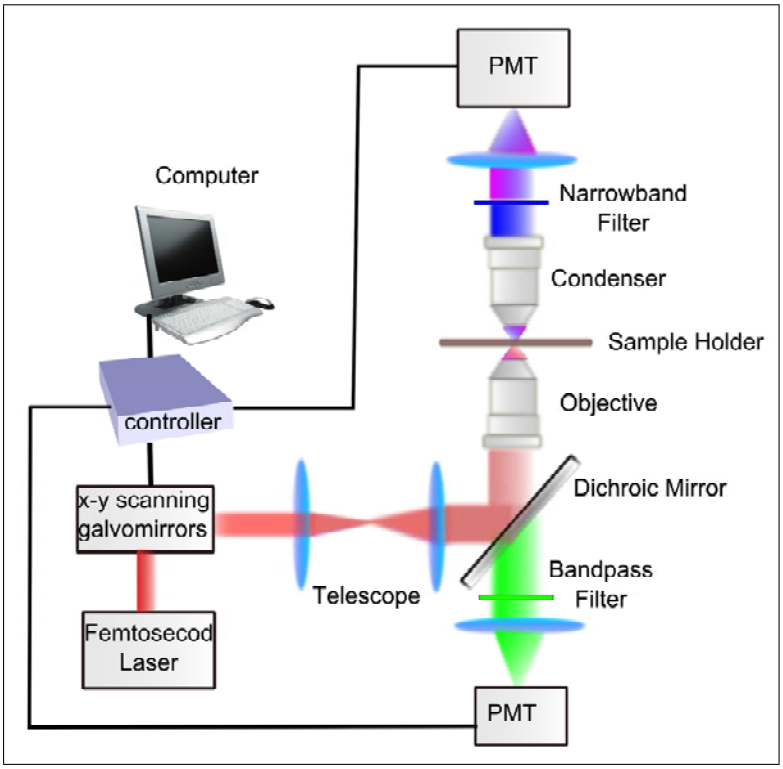

Figure 2.9: Schematic representation of a Multiphoton microscope

2.3.3 Third Harmonic Generation (THG) Microscopy

Like Second Harmonic Generation (SHG), Third Harmonic Generation is a parametric nonlinear process but of the third order. Here light of wavelength ω after interacting with a material yields an output light of frequency exactly triple the input ie. at 3ω. This process can be visualized in the Figure 2.10.

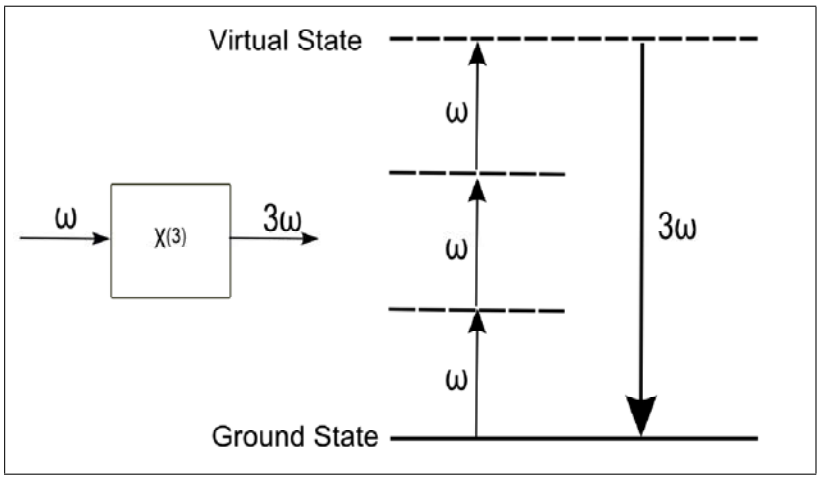

Figure 2.10: Process of Third Harmonic Generation (THG)

In THG three photons of frequency ω are destroyed and a single photon of frequency 3ω is simultaneously created in a single quantum mechanical process. As explained in Section 2.3.2 to describe SHG, THG can also be described using Equation 2.3 and an electric field considered as in Equation 2.4. If the third order nonlinear susceptibility is non zero then form Equation 2.3, the nonlinear polarization created in the crystal is given by:

$$\begin{aligned} \tilde{P}^{(3)}(t) &= \epsilon_0 \chi^{(3)} \tilde{E}^3(t) \\ &\equiv 3\chi^{(3)} E^2 E^* e^{-i\omega t} + (\chi^{(3)} E^3 e^{-i3\omega t} + c.c) \end{aligned} \tag{2.6}$$

It can be seen that the third-order polarization consists of a contribution at the fundamental frequency (the first term) and a contribution at frequency 3ω. The latter contribution can lead to the generation of radiation at the third-harmonic frequency.

Unlike SHG, THG depends on an odd order susceptibility. Odd order susceptibilities unlike even order susceptibilities donot vanish for a crystal with centrosymmetry. Hence THG can be produced even in crystals that have centrosymmetry. THG amplitude depends on the cube of the incident light intensity. This means that three photons need to arrive near simultaneously and hence THG requires a very large flux of excitation photons (higher than SHG) impinging on the sample. Since the THG intensity decreases as a power of three with decreasing excitation intensity, it provides greater intrinsic optical sectioning ability with a focused beam of incident optical excitation compared to SHG. Like the SHG signal, THG signal too travels preferentially in the forward direction for similar reasons as described in Section 2.3.2 for SHG.

It would seem form the above discussion that THG could be produced in any crystal. However when tightly focused laser beams, are used (as in multiphoton microscopy of biological specimens) the Gouy phase shift plays a spoil sport. A converging light wave experiences a $n\pi/2$ axial phase shift as it passes through its focus in propagating from $-\infty$ to $+\infty$ [58]. Here the dimension n equals 1 for a line focus (cylindrical wave) and equals 2 for a point focus (spherical wave) [58]. Hence when high numerical aperture objectives are used to excite THG, there is a π phase shift between the THG radiation created before and after the focus, which significantly reduces the efficiency of THG [39]. Qualitatively, in a homogeneous medium the THG waves generated before and after the focal point destructively interfere, which results in the absence of a net THG production [39]. However, in case of inhomogeneities near the focal point like in case of interfaces, efficient generation of the third harmonic is possible. A refractive index mismatch that leads to a positive phase mismatch condition $\triangle k = 3k_f - k_{th} > 0$ leads to efficient THG generation [39]. Here 'k' is the wave vector 'f' the fundamental frequency and 'th' is the third harmonic frequency.

Use of THG for microscopy

The contrast in THG microscopy is based on either a change in third-order susceptibility or in the dispersion properties of the material, within the focal volume of the fundamental radiation [39]. Hence THG can be efficiently used in imaging membranes of cells and organelles inside the cell. Since THG propagates preferentially in the forward direction the same laser scanning microscopy setup with a forward detection mount as used for SHG microscopy (Figure 2.9) can double as a THG microscope with proper choice of filters. Most lasers used for multiphoton microscopy however use wavelengths that would produce THG in the UV. Hence it is very important to select collection optics

that efficiently transmit these wavelengths or use special femtosecond laser systems that operate at wavelengths preferably above 1 micron.

One of the first reports of using THG microscopy was in 1997 when it was used to image a sample of optical glass fiber in an index matching oil [59]. A strong THG signal is generated at the fiber-oil interface. One of the first uses of THG for biological applications was the THG imaging of rhizoids from Chara plant [60]. THG microscopy has also been used to image neurons [61]. The plasma membrane in the cell body and the axons and the dendritic spines were imaged. In yeast cells the plasma membrane and membranes of internal organelles have been imaged [61]. In addition chloroplasts of leaves [62], Erythrocytes [62], calcium transients in glial cells [63], centrosomes, chorion surface, and interface between somites in zebrafish embryos [64], mouse bone [65], Xenopus laevis embryo [65], Drosophila egg chamber [65], sea-urchin larval spicules [65], lipid bodies [66], membranes in *C.elegans* [67], neurodegeneration in *C.elegans* [68] etc: have been imaged using THG microscopy.

2.3.4 Coherent Antistokes Raman Scattering (CARS) Microscopy

Coherent Antistokes Raman Scattering (CARS) is based on the Raman effect and allows imaging of vibrational levels which are characteristic signatures of certain molecules. When monochromatic light of frequency ω_P is incident on a material, the scattered light in addition to having a Rayleigh Scattered fundamental component (ω_P) also has weaker frequency components red or blue shifted with respect to ω_P [38]. The signals so generated $\omega_P \pm \omega_R$ are called Raman scattered components. The red-shifted frequencies are called the Stokes components and the blue-shifted frequencies called the anti-Stokes components [38]. The frequencies ω_R correspond to characteristic frequencies of molecular motions or the energy associated with vibration levels of the molecules and are most commonly vibrations of individual chemical bonds or groups of neighboring chemical bonds. Hence the spectrum obtained can be used to identify and characterize molecules. The stokes sifted components arise when the incident photons part away some energy to excite the molecule to a higher vibrational energy level and the anti-stokes shifted components arise when the incident photons gain some energy form the already vibrationally excited molecule.

Raman scattering is however inherently weak. Only 1 part out of 10^6 of the incident radiation will be scattered into the Stokes frequency when propagating through 1cm of a typical Raman active medium [38]. Very strong signals can however be produced using a coherent nonlinear Raman process. By using two light beams of frequencies ω_P and ω_S such that $\omega_P - \omega_S = \omega_R$, the vibrational Raman energy level with characteristic frequency ω_R can be excited. Here ω_P is called the pump frequency and ω_S the stokes frequency. The joint action of the Pump and Stokes fields act as a source for driving the Raman mode actively at the difference frequency $\omega_P - \omega_S$. Such driving creates a coherent superposition of molecular eigenstates, typically the ground state and a vibrationally excited state. Now if a third beam with frequency ω_{Pr}, called the probe, interacts with the same interaction volume as the pump and stokes beam, the coherent vibrational motion modulates the material properties such that it shifts the frequency of the probe optical field, with the vibrational frequency ω_R producing the CARS signal $\omega_{CARS} = \omega_{Pr} + \omega_R$. CARS can generate signals that are about 10^5 stronger than in spontaneous Raman scattering [38]. The process of CARS is schematically shown in Figure 2.11.

The CARS spectrum generally consists of both a resonant and a nonresonant contri-

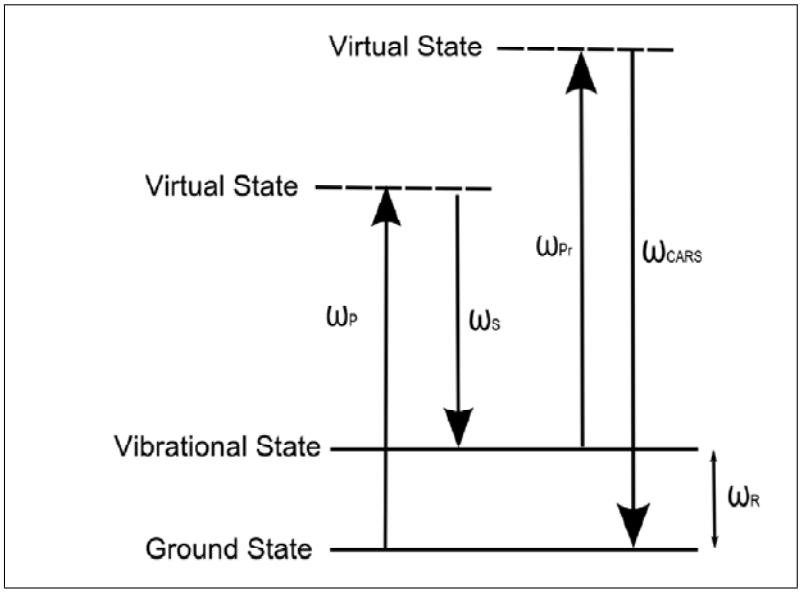

Figure 2.11: Process of Coherent Antistokes Raman Scattering (CARS)

bution. The resonant part is proportional to the square of the Raman scattering cross section [39]. It is a coherent process like SHG and THG and the CARS signal propagates preferentially in the forward direction determined by the phasematching geometry ($k_{AS} = k_P - k_S + k_{Pr}$), where 'k' is the wave vector [39]. Like THG the signal has a cubic dependence on the input excitation intensity and this provides intrinsic optical sectioning when the excitation beams are used under tight focusing conditions.

Use of CARS for microscopy

A laser scanning microscopy setup as used for SHG and THG microscopy with a forward detection arrangement (Figure 2.9) can also be used for CARS microscopy. However some modifications are necessary. The schematic of the CARS setup is shown Figure 2.12.

Two lasers (the pump laser and the stokes laser) are synchronized in time and made collinear before being focused by a high NA microscope objective onto the sample [39]. The lasers used can be picosecond and/or femtosecond for the pump and stokes lasers respectively. Many setups use a single laser system, with the second laser generated out of the first using an arrangement like the Optical Parametric Oscillator (OPO), which automatically takes care of the synchronization issue. The pump laser usually also doubles as the probe laser, which keeps the arrangement rather simple. The CARS image is acquired point-by-point where the sample is scanned in all three spatial directions [39].

The CARS signal is emitted preferentially in the forward direction and is collected using a forward collection system. The Pump and Stokes wavelengths are blocked by a set of appropriate filters. The collected signal is passed though a spectrometer that is used to observe a characteristic Raman peak corresponding to the chemical of interest, with typical acquisition times in the order of 20–100ms [39]. A 3D map of the intensity distribution of this peak gives the required CARS image that is essentially a spatial map of the distribution of the chemical of interest, in the sample under observation. In the mul-

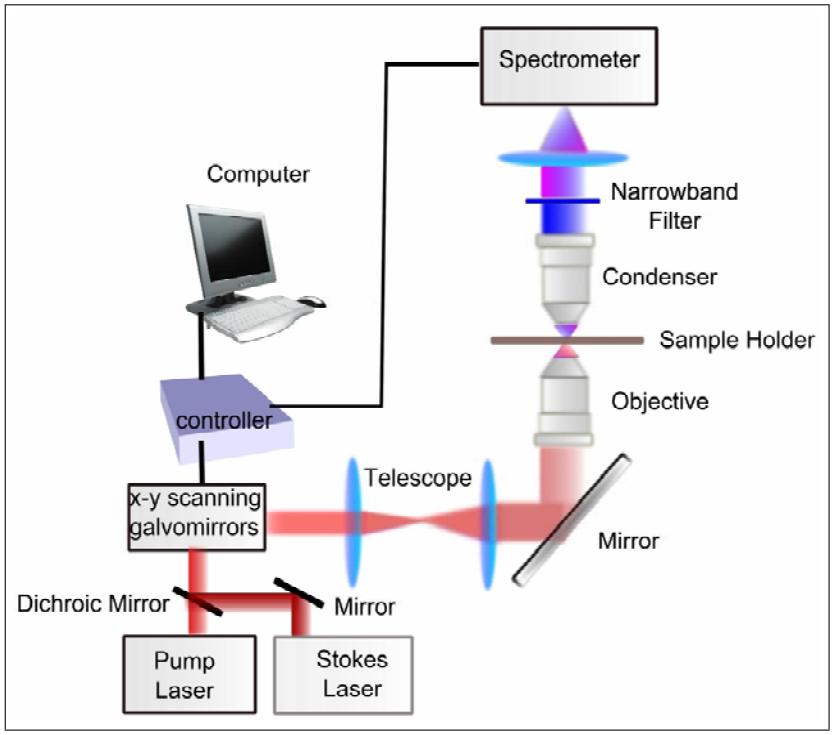

Figure 2.12: Schematic of Coherent Antistokes Raman Scattering (CARS) Microscope.

tiplex CARS configuration a narrow bandwidth ($\sim$2cm^{-1}) picosecond Ti:Sapphire Pump laser is used, in combination with a broad bandwidth ($\sim$150cm^{-1}) femtosecond tunable Ti:Sapphire Stokes laser [39].

CARS microscopy [69] has found many applications in imaging chemical and biological systems, especially since the CARS signal is intrinsic like SHG and THG and does not require the use of a contrast generating agent like a fluorophore in fluorescence microscopy. It has been used to visualize the thermodynamic state, either liquid crystalline or gel phase, of lipid membranes [70], diffusion of chemical compounds and lipid rich structures in mouse tissues [71], 3D distribution of chromosomes and vesicles surrounding the nucleus in unstained cells undergoing mitosis and apoptosis respectively [72], axonal myelin in live spinal tissues [73], organelle transport in living cells [74], lipid storage in *C.elegans* [75] etc:.

2.3.5 Ultrashort Laser Induced Nano-Surgery

The multiphoton microscope is a very versatile tool for imaging, however, when the mean power at the sample is increased to the range of 50 mW to 250mW and the pulse energy to 0.5nJ to 3nJ, destructive effects occur [76; 77]. At these power and pulse energy levels, the transient laser intensity reaches the TW/cm^2 range, which is sufficient to induce multiphoton ionization and plasma formation [38]. When working near the threshold for optical breakdown, material ablation can be realized within the central part of the diffraction-limited subfemtoliter multiphoton interaction volume without any collateral effects [76; 77]. Laser induced surgery has been conventionally performed using ultraviolet

CW or pulsed lasers [78–80]. Even though the UV wavelengths provide a small spot size at the focus, the laser induced damage extends beyond focus. This limits the degree of control in the region where damage is induced. Moreover UV light does not penetrate deep and hence surgery in thick tissues is seldom possible.

In contrast, the use of NIR ultrashort pulsed lasers, with their high light penetration depth on the order of several millimeters, allows precise intratissue surgery due to the lack of efficient absorbers in the 700nm to 1200nm spectral range [38]. Since the ablation\surgery takes place due to an essentially non-linear process, the effect is well confined within the focal spot, providing submicron accuracy in the surgical process. Volumes as small as 0.1 femtoliters can be ablated without damage to the surrounding regions [81].

With increasing numerical aperture the spot size becomes smaller, and thus the power that is necessary to overcome the threshold irradiance decreases. Beyond a certain numerical aperture, the breakdown power is smaller than the critical power for self-focusing, and localized energy deposition on a submicrometer scale can be achieved [82]. Nonlinear absorption of short and ultra-short laser pulses focused through microscope objectives of high numerical aperture (NA) hence can be used to achieve very fine and highly localized laser effects inside biological media that are transparent at low irradiance [82; 83].

Mechanisms of Femtosecond Laser Induced Nano-surgery

Confinement of multiphoton effects to the focal spot and the low energy threshold of femtosecond optical breakdown provides a very high degree of precision for femtosecond laser induced nanosurgery . Moreover the formation of plasmas with a large free-electron density in the femtosecond regime in a fairly large irradiance range below the breakdown threshold mitigates the mechanical effects such as shock wave formation and cavitation bubble formation, which other wise extend the induced damage far beyond the focal region [84].

The process of plasma formation essentially consists of the formation of quasi-free electrons by an interplay of photoionization and avalanche ionization. In multiphoton ionization even though a single photon does not have the energy to induce ionization a number of photons act together to promote the bound electron to a free state [85]. In tunneling ionization an electric field stronger than the coulomb potential that holds the electron in its orbit allows the tunneling of a bound electron to a free state [85].

Once a free electron is produced it absorbs incident photons by the non-resonant process of inverse Bremsstrahlung. The absorption of photon imparts kinetic energy to the electron and after a sequence of several inverse Bremsstrahlung absorption events, the kinetic energy is sufficiently large to produce another free electron through impact ionization [84]. These two low kinetic energy electrons can gain more energy through inverse Bremsstrahlung absorption. The recurring sequence of inverse Bremsstrahlung absorption events and impact ionization leads to an avalanche growth in the number of free electrons if the irradiance is high enough to overcome the losses of free electrons through diffusion out of the focal volume and through recombination [84]. This process eventually leads to plasma formation.

Once a very high density plasma is formed the incident laser light can be efficiently absorbed by electrons via free-carrier absorption. This intense heating of the electron plasma and the subsequent hydrodynamic expansion of the plasma cause permanent ma-

terial modification in condensed matter [85]. In case of femtosecond regime the seed electrons required for optical breakdown is provided by the high intensity whereas such seed electrons in pulses longer than 5 picoseconds is produced by impurities and defects in the material [85].

The temperature rise within a few picoseconds to tens of picoseconds in the focal volume during nanosurgery. This is time during which the thermalization of the energy carried by the free electrons takes place. This time interval is much shorter than the acoustic transit time from the center of the focus to its periphery and prevents any acoustic relaxation [84]. Hence there is a confinement of the the thermoelastic stresses caused by the temperature rise in the focal volume, leading to a maximum pressure rise [84]. In aqueous medium this gives rise to a cavitation bubble when the tensile strength of the material is exceeded. For cell surgery, the threshold for bubble formation defines the onset of disruptive mechanisms contributing to dissection [84].

There are two parameter regimes used for nanosurgery:

1. Using long series of pulses from fs oscillators with repetition rates of the order of 80 MHz and pulse energies well below the optical breakdown.

2. Using amplified pulses (typically 1KHz repetition rate) form a regenerative amplifier attached to a femtosecond oscillator. This regime uses pulse energies slightly above the threshold for transient bubble formation.

At repetition rates in the kilohertz range the mechanical and thermal events induced by subsequent pulses are largely independent however in the megahertz range accumulative effects are likely to occur [84]. Hence the possibility of thermally induced damage is higher when megahertz regime is employed.